

Junhong Wang\*

National Center for Atmospheric Research (NCAR)<sup>1</sup>, Boulder, Colorado

## 1. ABSTRACT

The dropsonde humidity data have not been fully utilized due to lack of knowledge of performance of the dropsonde humidity sensor. This study evaluates the performance of dropsonde humidity sensor using dropsonde data collected from three field experiments, DYCOMS-II (The Dynamics and Chemistry of Marine Stratocumulus Phase II: Entrainment Studies), IHOP (International H<sub>2</sub>O Project) and BAMEX (Bow Echo and Mesoscale Convective Vortex Experiment). The evaluation focuses on the dry bias suggested by previous studies, the performance within clouds and impacts of sensor wetting. Comparisons of dropsonde data with co-incident Vaisala radiosonde data during IHOP and BAMEX show good agreements and suggest no dry bias in the dropsonde data. The performance within clouds is evaluated using the data collected during DYCOMS-II, in which all 63 dropsondes went through marine stratocumulus clouds. The maximum RH inside clouds does not reach 100% all the time, but is within the sensor accuracy range (94-100%). The dropsonde humidity sensor experienced large time-lag errors when it descended from a dry environment above clouds into clouds. Mean estimated time constant of the sensor is 5 s at 15°C, which is much larger than 0.1 s at 20°C given by the manufacture. The sensor wetting effect exhibits in two ways. The humidity sensor still reported near-saturation RH after it exited clouds because of water on the sensor. When the dropsonde descended through a cloud or precipitation during BAMEX, the temperature profile shows rapid, unrealistic cooling right below cloud base, which is so-called "wet-bulb" effect and is due to the fact that the temperature sensor became wet.

## 2. INTRODUCTION

The NCAR GPS dropsonde system, also known as AVAPS (Airborne Vertical Atmospheric Profiling System), is currently installed on about 21 aircrafts around the world. Each year about 5000 dropsondes are dropped over data-sparse regions such as over oceans or

above remote mountain or polar regions to provide atmospheric thermo-dynamical and wind profiles. Since 1997, NOAA has used GPS dropsondes routinely during their hurricane reconnaissance flights to help predict the path and intensity of hurricanes. However, due to insufficient knowledge of performance of dropsonde humidity sensor, hurricane forecasters have not used the dropsonde humidity data to initialize their models. In addition, there have been increased demands of dropsondes over land for field experiments to map moisture and validate airborne remote sensors, such as IHOP and BAMEX. Previous limited studies suggest a dry bias of ~8%-20% in dropsonde humidity data (Kooi et al. 2002; Vance et al. 2002). Therefore, the goal of this paper is to evaluate the performance of dropsonde humidity sensor, provide evaluation results to dropsonde user community and build their confidence on dropsonde humidity data. The evaluation is carried out by comparing with co-incident radiosonde and aircraft in-situ humidity data.

## 2. INSTRUMENTATION AND FIELD EXPERIMENTS

**NCAR GPS Dropsonde:** A dropsonde is launched from aircrafts and descends through the atmosphere by a parachute to make measurements of pressure, temperature, humidity and wind. The NCAR lightweight digital GPS dropsonde was developed in 1995 and is currently manufactured by Vaisala Inc. under license from NCAR, so is also known as Vaisala dropsonde RD93 (Hock and Franklin 1999). The dropsonde includes a pressure, temperature, humidity sensor module (RSS903), a codeless GPS receiver module for wind measurements and a 400 MHz telemetry transmitter to transmit data from the sonde to the onboard receiving system (Fig. 1). Sensor specifications are given in Table 1. The aircraft data system includes a narrow-band 400 MHz telemetry receiver, which allows simultaneous operation of up to 4 dropsondes in the air. The dropsonde humidity sensor is the same as Vaisala RS90 H-HUMICAP thin film capacitor with twin-sensor design except that the alternative heating of twin sensors is turn off for dropsondes. The measurement from the lower humidity sensor (near the temperature sensor) is used in final data products.

The Revision D of the Vaisala RD93 dropsonde was introduced in April 2003; the predecessor was the Revision B dropsonde. The Rev D version is different

\* Corresponding author address: Dr. Junhong Wang, NCAR/ATD, P.O.Box 3000, Boulder, CO 80307-3000. Tel: 303-497-8837, Email: [junhong@ucar.edu](mailto:junhong@ucar.edu)

<sup>1</sup>The National Center for Atmospheric Research is sponsored by the National Science Foundation.

from the previous version (Rev B) in the lower part where the temperature and humidity sensor boom is mounted (Fig. 2). The lower part was redesigned to allow the use of a contamination shield over the sensor boom to eliminate the chemical contamination of the humidity sensor, which was also introduced in May 2000 for RS80 radiosondes (Wang et al. 2002). The lower bulkhead is made from two identical parts that combine to make a single sensor bulkhead piece which simplifies the manufacturing process. The lower sensor portion in the Rev B sonde has four elements, the outer tube, an inner reinforcement tube, sensor bulk head and an end cap.

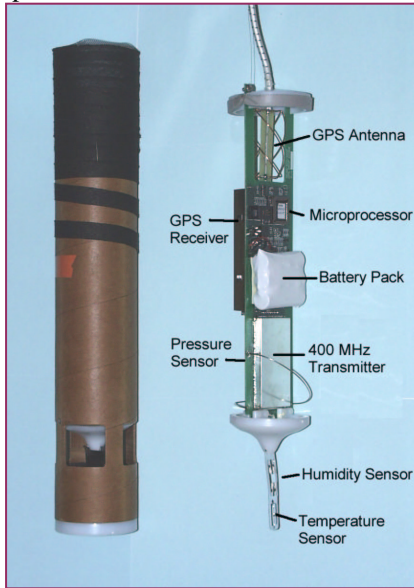


Fig. 1: The picture shows the actual dropsonde (left) and the design (right) with labels of each component. Courtesy of ATD for the picture.

Table 1: Specifications and accuracy for different instruments used in this study.

Instrument	Variables	Precision	Accuracy
Dropsonde	RH	1%	5%
	pressure	0.1 hPa	1.0 hPa
	temperature	0.1 °C	0.2 °C
	wind	0.1 m/s	±0.5 m/s
General Eastern 1011B Dew Point Hygrometer	dew point	0.006°C	±0.5 °C
	temperature		(>0 °C) ±1.0 °C (<0 °C)
PMS Liquid Water Sensor	liquid water content	0.001 g/m <sup>3</sup>	0.02 g/m <sup>3</sup>
Vaisala H-Humicap for radiosonde	RH	1%	5%

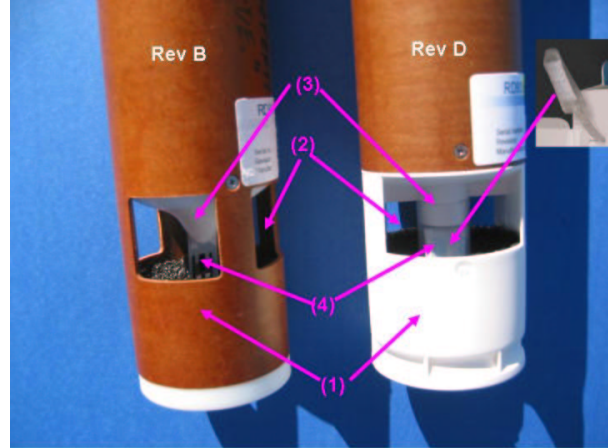


Fig. 2: Pictures of Rev B and Rev D dropsondes. Numeric labels show four major differences between two (see the text for details). The small inserted picture shows the contamination shield over the sensor boom in Vaisala RS80 radiosonde. A small bag of desiccant is inside the shield.

**DYCOMS-II:** The DYCOMS-II (The Dynamics and Chemistry of Marine Stratocumulus Phase II: Entrainment Studies) field program was designed to collect data to test large-eddy simulations of stratocumulus (Stevens et al. 2003). The experiment consisted of 9 NCAR EC-130Q flights out of North Island Naval Air Station between July 7 and July 28, 2001. Sixty-three NCAR GPS dropsondes were dropped from the NCAR EC-130Q on seven flights. The C130 was also equipped with a General Eastern 1011B dew point hygrometer and a PMS liquid water sensor (see Table 1).

**IHOP\_2002:** IHOP\_2002 (International H<sub>2</sub>O Project) took place over the Southern Great Plains (SGP) of the United States from 13 May to 25 June 2002 (Weckwerth et al. 2003). The main goal of IHOP\_2002 was improved characterization of the four-dimensional distribution of water vapor and its application to improving the understanding and prediction of convection. Six aircrafts were involved in the experiment; two of them, FII Learjet and DLR Falcon, were used for dropsondes. Total 420 NCAR GPS dropsondes were dropped for four different missions.

**BAMEX:** The BAMEX (Bow Echo and Mesoscale Convective Vortex Experiment) is a measurement campaign designed to investigate bow echoes, principally those which produce damaging surface winds and last at least 4 hours and larger convective systems which produce long lived mesoscale convective vortices (MCVs). The experiment was conducted from 20 May to 6 July 2003 in Illinois. Four hundred and thirty-eight NCAR GPS dropsondes were dropped from WMI Learjet on eighteen missions. New Vaisala RD93 Revision D dropsondes were dropped

during BAMEX for the first time (see above about Rev D dropsonde). Figure 3 shows all 438 dropsonde launch locations along with mobile Vaisala RS80-H radiosonde launch locations.

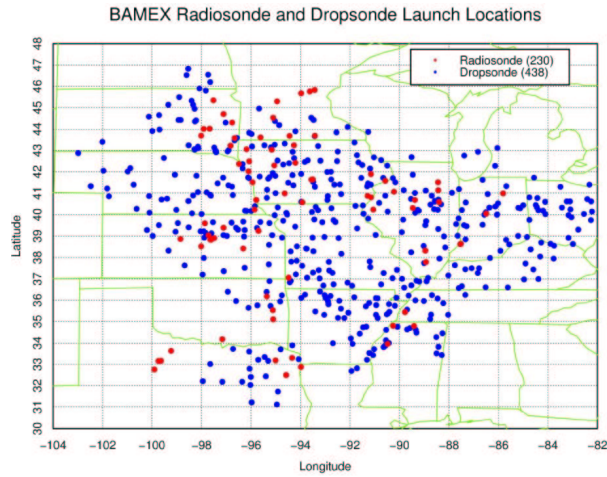


Fig. 3: Maps of dropsonde and radiosonde locations launched during BAMEX. Numbers of soundings are given in the parenthesis in the legend.

### 3. COMPARISON BETWEEN DROPSONDE AND COINCIDENT RADIOSONDE DATA DURING IHOP\_2002

The goal here is to take advantage of unprecedented water vapor data collected during IHOP to evaluate the performance of the dropsonde humidity sensor, focusing on the dry bias found by others. Wang et al. (2003) concluded that Vaisala radiosonde humidity sensors have good performance in the lower and middle troposphere, and thus can be used as a standard to validate dropsonde humidity sensor. Nine pairs of dropsonde and radiosonde soundings were launched within 20 km and a half hour during IHOP and are compared. The comparison shows good agreements between dropsonde and radiosonde data except when the dropsonde fell through strong moisture gradients (Fig. 4). When the dropsonde fell from a dry layer into a moist layer, such as moist layers around 800 mb for two soundings shown on the leftmost panel in Figure 4, the dropsonde humidity sensor is lagged behind the radiosonde, and the maximum RH inside moist layers is smaller than that from radiosonde data. However, the dropsonde data collected around the ARM central facility where Vaisala RS90 radiosonde was launched show very good agreements in RH and specific humidity with radiosonde data above and inside the moist layer (Fig. 4). Note that the dropsonde has the same humidity sensor as Vaisala RS90 radiosonde but without alternative heating of twin sensors. Mean difference between dropsonde and radiosonde RHs is within 2% except near the top of the boundary layer and

at ~4.4 km where strong moisture gradients occur, suggesting no systematic dry bias in dropsonde data (Fig. 5). The comparison between dropsonde humidity and airborne water vapor lidar data shows less than 5% difference with respect to the lidar value for mixing ratio (MR) for LearJet dropsonde data, but a dry bias of 0-10% in Falcon dropsonde data (Ed Browell, personal communications).

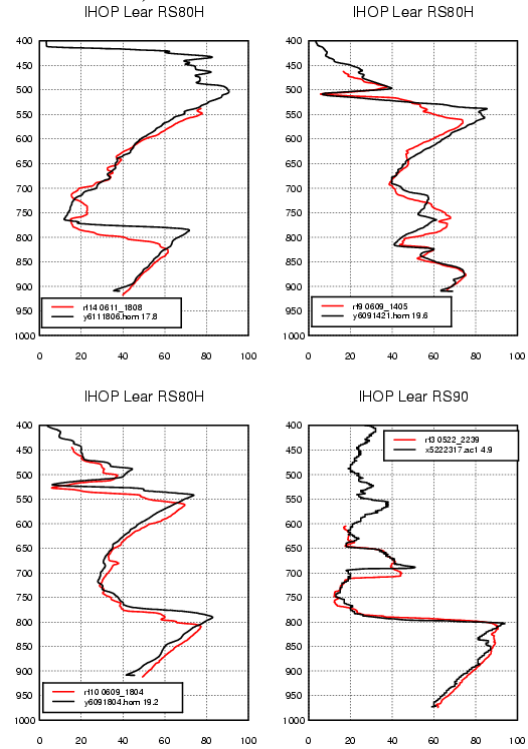


Fig. 4: RH (%) profiles from dropsonde data (red) and co-incident radiosonde data (black) for four cases. Vertical axes are pressure in hPa. The title illustrates whether Vaisala RS80-H or RS90 radiosondes were launched.

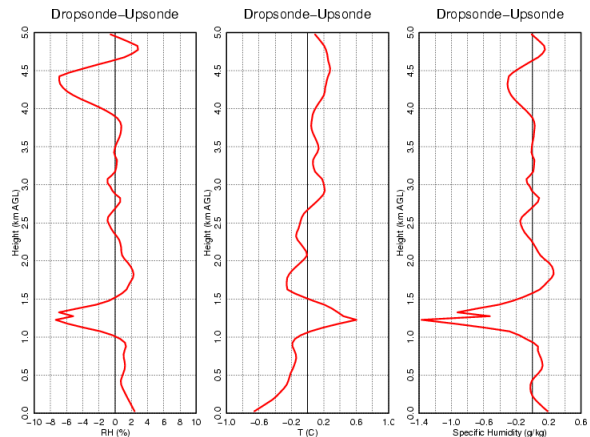


Fig. 5: Mean differences (Dropsonde-Radiosonde) of RH (%), temperature (°C) and specific humidity (g/kg) profiles averaged for nine cases.

Vaisala Humicap humidity sensor could have a dry bias if it has been stored for a long time due to the contamination from out-gassing of the sonde packaging material (Wang et al. 2002). During IHOP 105 dropsondes out of total 402 dropped from LearJet have PTU sensor module manufactured from one to three years ago; the rest of them were only about three to six months old. The comparison of old and new sondes launched within 50 km and a half hour is conducted. Unfortunately it is difficult to separate the difference due to sonde ages from real humidity variations, which occurred on very small spatial and temporal scales during IHOP. Figure 6 shows comparisons of RH profiles from four sondes launched within 20 km and 40 minutes in one flight on June 15, 2002. One of them (615\_200940) was 1.7 years old, but other three surrounding it were four to six months old. The comparison shows that this old one is drier than all other three. However, it is not conclusive about the dry bias and its magnitude of the old sonde because of real humidity variations.

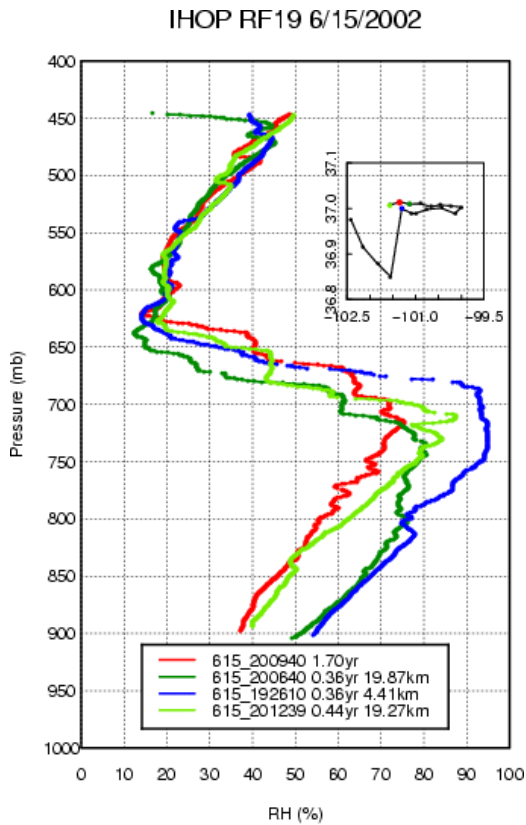


Fig. 6: Comparisons of RH profiles from four dropsondes launched within 20 km. The age of PTU sensor module is given in the legend. The number in km in the legend is the distance between the 615\_200940 sonde and others. The inserted plot shows launch locations of all dropsondes (big and color dots for four sondes shown in the figure).

#### 4. EVALUATION OF PERFORMANCE IN CLOUDS USING DYCOMS-II DATA

During DYCOMS-II, 63 dropsondes were dropped into marine stratocumulus clouds. Temperature and RH profiles of all soundings show the presence of moist layers (RH > 90%) in the boundary layer for all missions and temperature inversion layers above these moist layers (Fig. 7). It suggests that these moist layers are marine stratocumulus cloud layers. RHs inside moist layers can vary from 90% to 100%, indicating potential problems of humidity sensor to report 100% RH. However, the maximum RH of each profile for all soundings ranges from 94% to 100%, which is consistent with 5% of the sensor accuracy (see Table 1), and about 28% of them have the maximum RH of 100% (Fig. 8). This suggests that the dropsonde data do not have systematic dry bias near saturation.

The flight altitude pattern of Research Flight (RF) 1 is given in Figure 9 and represents typical ones for other flights. The RH profile measured by the GE DPH during the ascending is compared with the nearby dropsonde profile; the LWC profile measured by the PMS is used to identify cloud top and base locations (Fig. 9). The descending profile shown in Figure 9 can not be used because of poor performance of the GE DPH during the descending, where the sensor experienced large RH transition. The comparison of RH profiles from dropsonde and GE DPH data shows two types of errors in dropsonde humidity data: the time lag error near the top of the cloud layer and the moist bias below cloud (Fig. 10).

Time lag errors in dropsonde and radiosonde data are well known in principle and are caused by the failure of sensors to respond instantaneously to changes in environment during descend or ascent. The sensor time constant is essential to correct time lag errors. The time constant provided by the manufacture is based on the laboratory test and can be easily different from that in the real world. The descending of dropsondes from the dry air above clouds into cloud layers provides an opportunity to estimate the time constant. Dropsonde-measured RH ( $RH_{m_i}$ ) can be expressed as:

$$RH_{m_i} = RH_c - \Delta RH * e^{t_i/\tau} \quad (1)$$

$$\Delta RH = RH_c - RH_0 \quad (2)$$

where  $RH_0$  is RH of the dry air above cloud (referred as RH at  $t_i = t_{ac}$ ),  $RH_c$  is dropsonde-measured RH inside cloud (referred as RH at  $t_i = 0$ ),  $t_i$  is the time from the cloud top, and  $\tau$  is the time constant. The time constant can be derived from (1):

$$\tau = t_i / \ln ((RH_c - RH_{m_i}) / \Delta RH) \quad (3)$$

In this study,  $\tau$  is calculated from the level where the humidity sensor reaches the equilibrium with the environment to the top of the temperature inversion. The former is the level at  $t_i = 0$  and is cloud top

determined by dropsonde RH profile using the same analysis method as in Wang and Rossow (1995) except using 94% RH threshold. The top of the temperature inversion is the level at  $t_i = t_{ac}$ , is determined by dropsonde temperature profile, and represents the location of the dry air right above cloud. For each sounding, multiple  $\tau$  values are derived using (3) from  $t_i = 0$  to  $t_i = t_{ac}$ , but have minor variations. For 50 soundings used to derive  $\tau$ , mean  $\tau$  value of each sounding ranges from 4 s to 8 s, but is from 4 s to 6 s for 90% of soundings. The estimated time constant of the dropsonde humidity sensor at cloud top that has a mean temperature of 15°C is 5 s, while the time constant given by manufacture is 0.1 s.

The moist bias below cloud shown in Figure 10 is due to the wetting of the humidity sensor after it exited out of cloud. The time for the sensor to evaporate water is defined as the time from LWC-determined to dropsonde RH-estimated cloud bases and is referred as the evaporation time. Figure 11 suggests that this evaporation time increases with cloud physical thickness and liquid water path (LWP) with correlation coefficients of 0.6 and 0.56, respectively. The alternative heating of twin humidity sensors (not currently implemented in dropsonde) might help speeding up evaporation of the water.

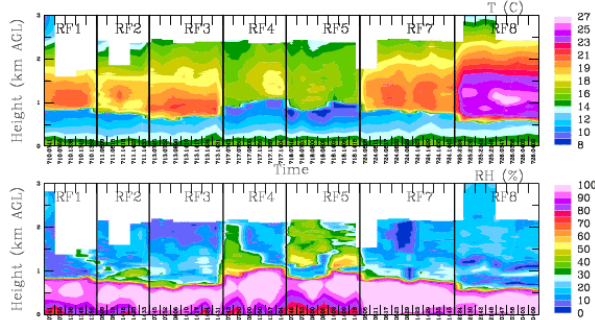


Fig. 7: Temperature and RH profiles for all dropsondes launched during DYCOMS-II. Mission names are given in the legend.

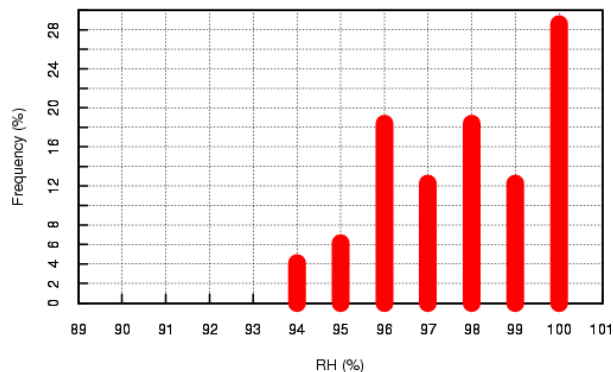


Fig. 8: Frequency of maximum RHs of each profile during DYCOMS-II.

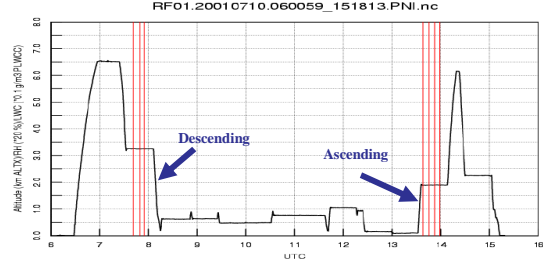


Fig. 9: RF1 flight altitudes (black line) as a function of UTC and dropsonde launch times (red vertical lines).

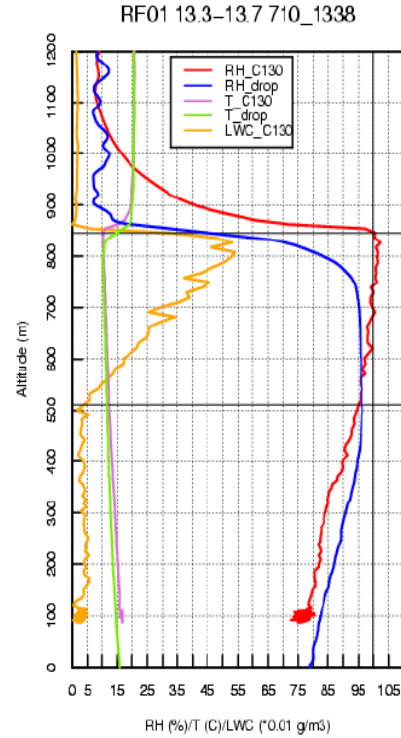


Fig. 10: RH and temperature profiles from dropsonde and GE DPH and PMS-measured LWC profile. Black lines denote cloud top and base determined by the LWC profile.

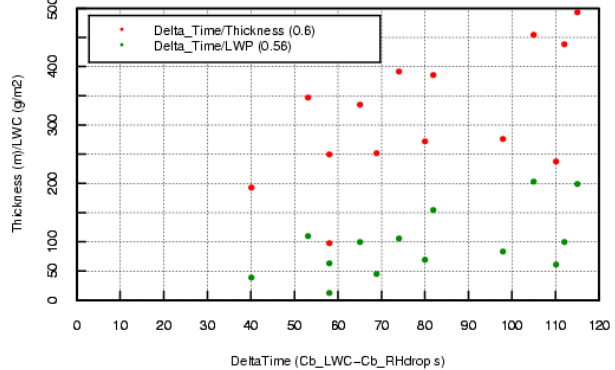


Fig. 11: Scatter plot of cloud physical thickness (red) and LWP (green) versus the evaporation time. Correlation coefficients are given in the legend.

## 5. EVALUATION USING BAMEX DATA

During BAMEX, 230 Vaisala RS80-H radiosondes were launched from three mobile radiosonde systems. Eight pairs of dropsonde and radiosonde soundings were launched within 50 km and a half hour, and therefore can be compared. The visual examination shows that for five pairs of them radiosonde and dropsonde were nearly sampling the same air mass. Comparisons of RH and specific humidity profiles in Figure 12 show good agreements between dropsonde and radiosonde humidity data, especially for specific humidity. Discrepancies of some small features might be due to the fact that two sondes sampled different air masses since the humidity can vary a lot on small spatial and temporal scales.

When the dropsonde descended through a cloud or precipitation, the temperature profile shows rapid, unrealistic cooling right below cloud base (see four examples in Fig. 13). This is another impact of the sensor wetting, is so-called "wet-bulb" effect and is due to the fact that the temperature sensor became wet. When the sensor was exposed to drier air below cloud, the water on the temperature sensor began to evaporate, causing the temperature to cool rapidly. It is not clear whether the new design of the Rev D sonde makes it easier for the temperature sensor to get wet.

## 6. CONCLUSIONS

The performance of the dropsonde humidity sensor is evaluated by comparing dropsonde data with coincident radiosonde and aircraft data collected from three field experiments. Based on the evaluation, three conclusions are drawn. (1) No systematic dry bias is found in dropsonde humidity data as suggested by previous studies. (2) Mean estimated time constant of the dropsonde humidity sensor, which is essential for correcting time lag errors, is 5 s at 15°C, while the time constant at 20°C given by the manufacture is 0.1 s. The estimated time constant will be applied to IHOP data to see how the time lag correction improves comparisons between dropsonde and radiosonde data at the top of the boundary layer. (3) As a result of wetting of the humidity sensor, the dropsonde overestimates RHs below clouds. Preliminary study suggests that the time taken to evaporate water on the sensor depends on cloud thickness and LWP. We recommend implementing alternative heating of twin humidity sensors to speed up the evaporation in the future. This study also reveals known wet-bulb effect due to the wetting of the temperature sensor.

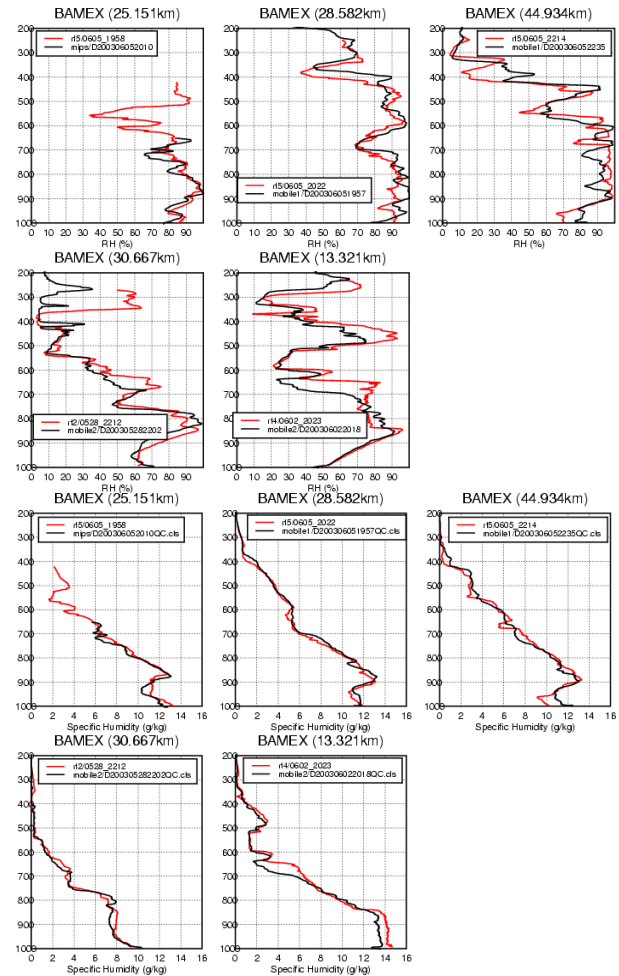


Fig. 12: Comparisons of RH and specific humidity profiles for five pairs of dropsonde (red) and radiosonde (black) soundings. Vertical axes are pressure in hPa. File names are shown in the legend

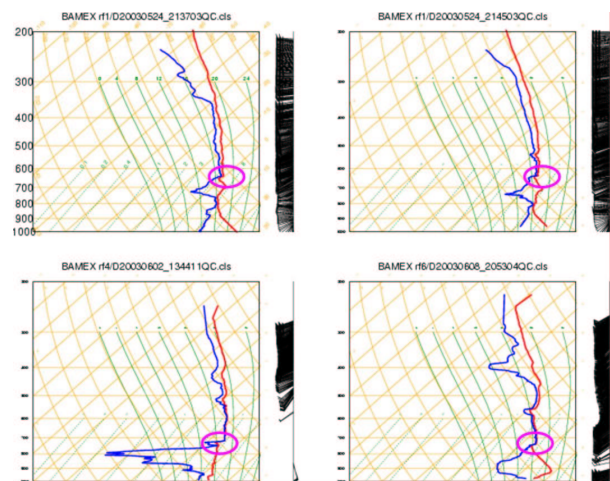


Fig. 13: Skew-T plots (red: temperature, blue: dew-point temperature) of four soundings with "wet-bulb" effects. Magenta circles highlight where wet-bulb effects took place.

## 7. ACKNOWLEDGMENTS

I would like to thank Matthew Coleman and Kate Beierle for helps with some of analyses, Terry Hock, Dean Lauritsen, Hal Cole and Krista Laursen for useful discussions.

## 8. REFERENCES

Hock, T. F., and J. L. Franklin, 1999: The NCAR GPS dropwindsonde. *Bull. Amer. Meteor. Soc.*, **80**, 407-420.

Kooi, S. A., R. A. Ferrare, S. Ismail, E. V. Browell, M. B. Clayton, V. G. Brackett, and J. Halverson, 2002: Comparison of LASE water vapor measurements with dropwindsonde measurements during the third and fourth Convection And Moisture Experiments (CAMEX-3 and CAMEX-4). Extended abstract for "International Laser Radar Conference".

Stevens, B., and co-authors, 2003: Dynamics and chemistry of marine stratocumulus – DYCOMS-II. *Bull. Amer. Meteor. Soc.*, **84**, 579-593.

Vance, A. K., J. P. Taylor, and T. J. Hewison, 2002: Comparison of in-situ humidity data from aircraft, dropsonde and radiosonde. *J. Atmos. Oceanic Technol.*, submitted.

Wang, J., H. L. Cole, D. J. Carlson, E. R. Miller, K. Beierle, A. Paukkunen, and T. K. Laine, 2002: Corrections of humidity measurement errors from the Vaisala RS80 radiosonde - Application to TOGA COARE Data. *J. Atmos. Oceanic Technol.*, **19**, 981-1002.

Wang, J., and W. B. Rossow, 1995: Determination of cloud vertical structure from upper-air observations. *J. Appl. Meteor.*, **34**, 2243-2258.

Wang, J., D. J. Carlson, D. B. Parsons, T. F. Hock, D. Lauritsen, H. L. Cole, K. Beierle, and N. Chamberlain, 2003: Performance of operational radiosonde humidity sensors in direct comparison with a reference-quality humidity sensor and its climate implication. *Geophys. Res. Lett.*, **30**, 10.1029/2003GL016985.

Weckwerth, T. M., D. B. Parsons, S. E. Koch, J. A. Moore, M. A. Lemone, B. B. Demoz, C. Flamant, B. Geers, J. Wang, and W. F. Feltz, 2003: An overview of the International H<sub>2</sub>O Project (IHOP\_2002) and some preliminary highlights. *Bull. Amer. Meteor. Soc.*, in press.